# Symmetry-enhanced spectral analysis via the spectral method and filter diagonalization

Rongqing Chen and Hua Guo*
*Department of Chemistry, University of Toledo, Toledo, Ohio 43606*
(Received 6 February 1998)

A symmetry-adapted propagation scheme is introduced to enhance the efficiency of spectral analysis using either the spectral method or filter diagonalization. The essence of the method is to project out symmetry components from a *single* wave packet that contains all the symmetry species. These components are then used to recover the spectrum and/or energy wave functions for each symmetry species. The adaptation of symmetry not only facilitates the symmetry assignment of the eigenstates, but also reduces the number of propagation steps because the density of states for individual symmetry species is typically much lower than that of the overall spectrum. Our approach is numerically superior to the conventional symmetry-adapted methods because the propagation of multiple wave packets is avoided. A simplified atomic model with two one-dimensional electrons is used as a numerical example. [S1063-651X(98)11506-4]

PACS number(s): 02.70.−c, 31.15.−p, 03.65.−w

## I. INTRODUCTION

Recently, there has been a proliferation of propagation based methods in quantum dynamical and spectroscopic calculations [1,2]. Within such a method, a series of propagation states, or wave packets, is generated by a propagation scheme: $|\Psi_k\rangle = \hat{U}_k(\hat{H})|\Psi_0\rangle$ where $|\Psi_0\rangle$ is an initial wave packet and $\hat{U}_k(\hat{H})$ is a generalized propagator. For time propagation on a uniform grid, $t_k = k\tau$ where $k$ is an integer, the propagator is defined as $\hat{U}_k(\hat{H}) = e^{-i\hat{H}t_k}$ (atomic units are used throughout the paper unless stated otherwise). In a polynomial propagation [2,3], such as the Chebyshev [4] or Lanczos propagation [5], the propagator is a $k$th order polynomial of the Hamiltonian $\hat{H}$. The propagation states are then used to recover energetic and/or temporal information of the system [4,6–11]. Typically, the major operation in a propagation based method is matrix-vector multiplication, which has favorable scaling laws in both cpu and memory requirements. In many cases, the Hamiltonian matrix is sparse and can be generated on the fly.

In this work, we concentrate on the determination of eigenenergies and eigenstates for quantum systems, but the method introduced here can be easily adopted for other quantum mechanical problems. There are two common approaches in spectral analysis. The spectral method [12,13] takes advantage of the unitary transformation between the energy domain and the generalized time domain [3]. A well-known example is the exponential Fourier transform between energy and time [14]. For the Chebyshev propagator, its angle (i.e., the effective energy) domain is related to its order (i.e., the effective time) domain by a cosine Fourier transform [4]. The spectrum and eigenstates of a system can be determined via the appropriate transformation from the correlation function and the propagation states, respectively. In the spectral method, the energy resolution is inversely proportional to the number of propagation steps (i.e., the uncertainty principle).

An alternative approach is the method of filter diagonalization [15,16]. The strategy here is to combine relatively short propagation with a variational solution of the eigenproblem in a small space. To this end, a number of filtered states in a prespecified energy range is first assembled from the propagation states using the spectral method. These energetically localized states are then used as primitive bases to construct the Hamiltonian matrix. Finally, the eigenproblem is solved by diagonalizing the Hamiltonian in the relatively small subspace spanned by the filtered states. It has been argued [17] that the spectral method can be regarded as a special case of filter diagonalization in which a single filter is used. The convergence of filter diagonalization still depends on the number of propagation steps, but the final diagonalization can greatly improve the resolution. Filter diagonalization is ideal for extracting eigenvalues and eigenstates in a given energy range [15–21]. If one is only interested in the spectrum in this range, the correlation function alone is sufficient to construct the Hamiltonian matrix and the explicit calculation and storage of the filtered states are unnecessary [22–25].

When the system under investigation possesses symmetry, the above schemes can be modified to improve efficiency. In the pioneering work of Feit *et al.* [13], for example, three symmetry-adapted wave packets were propagated to take advantage of the threefold rotational symmetry of the Hénon-Heiles system. Each propagation generates a spectrum in the corresponding symmetry. A similar strategy was taken in a recent study of acetylene by Liu and Muckerman [26]. The advantage of such a symmetry-adapted approach is obvious. According to the uncertainty principle, the resolution of a spectrum is inversely proportional to the number of propagation steps. The breakdown of the spectrum into symmetry species is likely to reduce the density of states and thus the number of propagation steps. Furthermore, it often occurs that energy levels with different symmetries form nearly degenerate clusters in the spectrum. Under such circumstances, the symmetry-adapted approach represents a natural and efficient way to remove the multi-

*Address after July 1, 1998: Department of Chemistry, University of New Mexico, Albuquerque, NM 87131.

 

plicity and to assign symmetry to the energy levels. The strategy is similar to the symmetry decomposition of the Hamiltonian matrix in direct diagonalization. The computational savings can be significant for highly excited states and for large systems. However, such an approach comes at a price of propagating multiple wave packets.

The method suggested here retains the same spirit as the conventional symmetry-adapted method mentioned above, but differs in that only a single wave packet needs to be propagated. All the symmetry components are projected out from this wave packet at each propagation step, thanks to the commutability between the symmetry operators and the system Hamiltonian. Our method thus has the same accuracy as the multiple wave packet method, but much less computational costs. In the next section, the method is presented in more detail. In Sec. III, a simplified multielectron atomic model is employed to illustrate its applicability and efficiency. The conclusion is presented in Sec. IV.

## II. THEORY

We seek, using propagation based methods, the efficient solution of the time-independent Schrödinger equation

$$\hat{H}|E_n\rangle = E_n|E_n\rangle, \tag{1}$$

where $E_n$ and $|E_n\rangle$ are the discrete eigenvalues and the corresponding eigenstates of the system Hamiltonian $\hat{H}$, respectively. The direct diagonalization approach is rejected because of its inefficiency for large problems. We further consider a physical system belonging to a symmetry group $S$ that contains $d_S$ symmetry operators $\hat{s}_i \in S$ with $i = 1,2,...,d_S$. By definition, a symmetry operator commutes with the Hamiltonian of the same system: $\hat{s}_i\hat{H} = \hat{H}\hat{s}_i$. In other words, it is always possible to find common eigenstates for both the Hamiltonian and the symmetry operators. Further, the symmetry operators should also commute with the propagator, $\hat{s}_i\hat{U}_k(\hat{H}) = \hat{U}_k(\hat{H})\hat{s}_i$, because $\hat{U}_k(\hat{H})$ is an operator function of $\hat{H}$. Therefore, symmetry properties of a wave packet are conserved during propagation. In the method used by Feit *et al.* [13], multiple symmetry-adapted initial wave packets were constructed by symmetrization. The propagation of each wave packet results in an independent series of propagation states that can be used to generate the symmetry-adapted spectrum. This strategy is more efficient than the single wave packet propagation with no symmetry adaptation.

In our method, a single wave packet is propagated and the symmetry-adapted propagation states are obtained at every propagation step by projection. The initial wave packet is designed to contain all the symmetry species,

$$|\Psi_0\rangle = \sum_{m=1}^{M} a_m|\Psi_0^{(m)}\rangle, \quad a_m \neq 0, \tag{2}$$

where $M$ denotes the number of symmetry species, or irreducible representations, belonging to the symmetry group $S$. The symmetry-adapted initial wave packets, which are the eigenstates of the corresponding symmetry operators, can be obtained by using symmetry projection operators

$$|\Psi_0^{(m)}\rangle = \hat{P}_m|\Psi_0\rangle. \tag{3}$$

The construction of the projection operators is well documented [27]. A projection operator $\hat{P}_m$ also commutes with the Hamiltonian and the propagator since it is a linear combination of the symmetry operators $\hat{s}_i$. As a result, the propagation does not mix different symmetry species. The $k$th step symmetry-adapted propagation states can be obtained by the projection of a single wave packet:

$$\begin{aligned}|\Psi_k^{(m)}\rangle &\equiv \hat{U}_k(\hat{H})|\Psi_0^{(m)}\rangle = \hat{U}_k(\hat{H})\hat{P}_m|\Psi_0\rangle \\ &= \hat{P}_m\hat{U}_k(\hat{H})|\Psi_0\rangle = \hat{P}_m|\Psi_k\rangle.\end{aligned} \tag{4}$$

In other words, a single wave packet gives rise to $M$ symmetry-adapted propagation states.

Often, correlation functions are the only quantities needed in spectral analysis. Thus, $M$ symmetry-adapted correlation functions can be calculated from a single propagation

$$C_k^{(m)} = \langle\chi^{(m)}|\Psi_k^{(m)}\rangle = \langle\chi^{(m)}|\Psi_k\rangle = \langle\chi|\Psi_k^{(m)}\rangle, \tag{5}$$

where the idempotency of the projection operator, $(\hat{P}_m)^2 = \hat{P}_m$, is used for the second and third parts of the equation. The state $|\chi^{(m)}\rangle$ can be arbitrarily chosen provided it has the appropriate symmetry, but it is typically given by the symmetry-adapted initial wave packet $|\Psi_0^{(m)}\rangle$. In this case, Eq. (5) yields the autocorrelation function. According to Eq. (5), the correlation function can be calculated in one of the three forms. If the projection can be done with minimal computational resources, the first or the third form is preferred for reasons that become clear below. In cases where the projection is expensive, the second form is numerically favored because only the initial state needs symmetrization.

The efficiency of the method can be further improved if one can take advantage of the inherent symmetry of the propagator. For example, the length of a time autocorrelation function can be doubled because $C_{2k} \equiv \langle\Psi_0|\Psi_{2k}\rangle = \langle\Psi_k|\Psi_k\rangle$ and $C_{2k-1} = \langle\Psi_{k-1}|\Psi_k\rangle$ [28]. Similar savings can be achieved for the Chebyshev propagation $[\hat{U}_k(\hat{H}) = \cos(k \arccos \hat{H})]$ as well [4,22]:

$$C_{2k-j} = 2\langle\Psi_{k-j}|\Psi_k\rangle - C_j \qquad \text{for} \quad j = 0,1. \tag{6}$$

However, such extensions can only be applied when the symmetry-adapted propagation states are explicitly projected out at all the steps. If the second part of Eq. (5) is used to calculate the correlation function, no such saving is permitted.

The symmetry-adapted propagation states and correlation functions can be subsequently employed to determine the eigenvalues and eigenstates via either the spectral method or filter diagonalization. In this work, the eigenproblem is solved for a prespecified energy range using a low storage version of the filter-diagonalization method [22–25]. Specifically, a generalized eigenequation

$$HB = ESB \tag{7}$$

is solved using an EISPACK routine [29]. The Hamiltonian $(H)$ and overlap $(S)$ matrices in a subspace spanned by the filtered states $|\Psi(E_l)\rangle = F(\hat{H}|E_l)|\Psi_0\rangle$ can be obtained di-

rectly from the autocorrelation function with no explicit computation of the filtered states [25]

$$H_{ll'}=\langle\Psi(E_l)|\hat{H}|\Psi(E_{l'})\rangle = \sum_{m=0}^{2K-1} F(E_m|E_l)E_m F(E_m|E_{l'})G(E_m), \tag{8a}$$

$$S_{ll'}=\langle\Psi(E_l)|\Psi(E_{l'})\rangle = \sum_{m=0}^{2K-1} F(E_m|E_l)F(E_m|E_{l'})G(E_m), \tag{8b}$$

where $K$ is the number of Chebyshev propagation steps. The spectral function is expressed as a discrete cosine Fourier transform of the autocorrelation function in the Chebyshev order domain

$$G(E_m)=\sum_{k=0}^{2K-1}(1-\delta_{k0}/2)\cos(k\ \arccos\ E_m)C_k, \tag{9}$$

and $\{E_m\}$ are the Gauss-Chebyshev quadrature points. For more details of the method, confer Ref. [25].

Since our approach propagates only a single wave packet yet provides an equal amount of information, the computational cost for the propagation is significantly reduced compared with the multiple wave packet approach of Feit *et al.* [13]. This is most conspicuous for systems with large $M$.

## III. MODEL AND RESULTS

To numerically test the method proposed in the previous section, we used a simple atomic model consisting of two one-dimensional spinless electrons [30]. This model has been used to study multiphoton ionization of multielectron atoms in intense laser fields [30,31]. The Hamiltonian of the system is given below

$$\hat{H}=-\frac{1}{2}\frac{\partial^2}{\partial x_1^2}-\frac{1}{2}\frac{\partial^2}{\partial x_2^2}-\frac{2}{\sqrt{\varepsilon+x_1^2}}-\frac{2}{\sqrt{\varepsilon+x_2^2}} + \frac{2}{\sqrt{\varepsilon+(x_2-x_1)^2}}, \tag{10}$$

where $\varepsilon=0.55$.

Obviously, the system has the following symmetry operations: the permutation between the two electrons $[\hat{s}_1:(x_1,x_2)\rightarrow(x_2,x_1)]$ and the inversion of the two coordinates $[\hat{s}_2:(x_1,x_2)\rightarrow(-x_1,-x_2)]$. Thus, the symmetry group contains four elements: $S=\{\hat{1},\hat{s}_1,\hat{s}_2,\hat{s}_1\hat{s}_2\}$ since $\hat{s}_1^2=\hat{s}_2^2=\hat{1}$ and $\hat{s}_1\hat{s}_2=\hat{s}_2\hat{s}_1$. Given an arbitrary wave function $\Psi(x_1,x_2)$, four symmetry species can be constructed:

$$\Psi^{(++)}(x_1,x_2)=[\Psi(x_1,x_2)+\Psi(x_2,x_1)+\Psi(-x_1,-x_2)+\Psi(-x_2,-x_1)]/4, \tag{11a}$$

$$\Psi^{(+-)}(x_1,x_2)=[\Psi(x_1,x_2)+\Psi(x_2,x_1)-\Psi(-x_1,-x_2)-\Psi(-x_2,-x_1)]/4, \tag{11b}$$

$$\Psi^{(--)}(x_1,x_2)=[\Psi(x_1,x_2)-\Psi(x_2,x_1)-\Psi(-x_1,-x_2)+\Psi(-x_2,-x_1)]/4, \tag{11c}$$

$$\Psi^{(-+)}(x_1,x_2)=[\Psi(x_1,x_2)-\Psi(x_2,x_1)+\Psi(-x_1,x_2)-\Psi(-x_2,-x_1)]/4, \tag{11d}$$

where the superscripts of the symmetrized wave functions $\Psi^{(s_1s_2)}$ denote the sign of the eigenvalues of the permutation and inversion operators

$$\hat{s}_1\Psi^{(s_1s_2)}=s_1\Psi^{(s_1s_2)},\quad \hat{s}_2\Psi^{(s_1s_2)}=s_2\Psi^{(s_1s_2)}. \tag{12}$$

Similarly, four symmetry-adapted autocorrelation functions can be defined [cf. Eq. (5)].

In our numerical test reported here, a square Fourier grid was used for the two coordinates: 512 points are evenly distributed in $[-80$ a.u. 80 a.u.$]$ for both $x_1$ and $x_2$. The Cartesian coordinate system is capable of reflecting the inherent symmetry of the system. The spectral span of the discretized Hamiltonian with a kinetic energy truncation of 20 a.u. is approximately between $-3$ and 22 a.u., which is rescaled to $[-1,1]$ for the Chebyshev propagator. The spatial grid is certainly insufficient to converge high Rydberg states due to the long range Coulomb tail. However, our main concern in this work was on how the filter diagonalization can be enhanced by the symmetry adaptation. Hence, the discretized

TABLE I. The lowest 20 eigenenergies of the model atom.

| $n$ | $E_n$ (a.u.) | $s_1s_2$ |
|---|---|---|
| 1 | −2.896990 | ++ |
| 2 | −2.297258 | −− |
| 3 | −2.163914 | +− |
| 4 | −2.096496 | −+ |
| 5 | −2.078994 | ++ |
| 6 | −2.026408 | −− |
| 7 | −2.007633 | +− |
| 8 | −1.989979 | −+ |
| 9 | −1.985736 | ++ |
| 10 | −1.970025 | −− |
| 11 | −1.963992 | +− |
| 12 | −1.957250 | −+ |
| 13 | −1.955622 | ++ |
| 14 | −1.949004 | −− |
| 15 | −1.946340 | +− |
| 16 | −1.943111 | −+ |
| 17 | −1.942322 | ++ |
| 18 | −1.938927 | −− |
| 19 | −1.937495 | +− |
| 20 | −1.935915 | −+ |

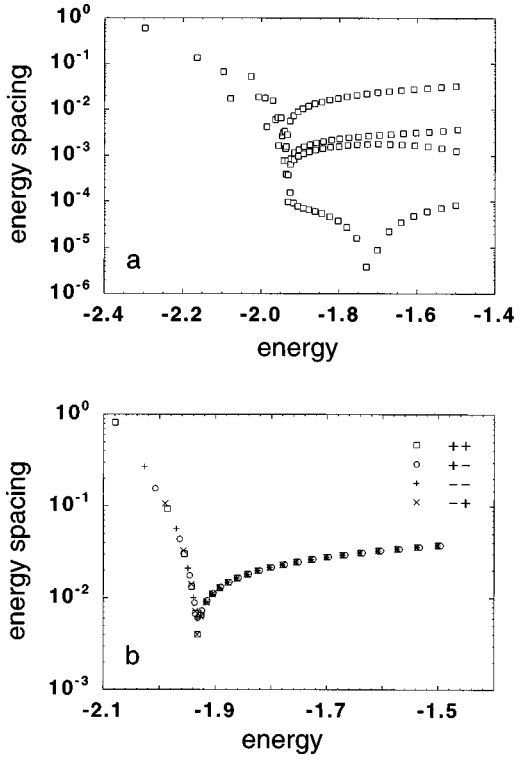


FIG. 1. Energy gaps as functions of energy for (a) the overall spectrum and (b) the symmetry-adapted spectra. The energy is given in a.u.

Hamiltonian merely serves as a numerical prototype. The action of the Hamiltonian onto a wave packet was evaluated using the fast Fourier transform method [13,32]. The eigenvalues in the range $[-3$ a.u., $-1.5$ a.u.$]$ were determined using the filter-diagonalization method outlined in the last section. Specifically, a wave packet containing all the symmetry species was propagated in the Chebyshev order domain [4]. Autocorrelation functions were calculated for the original wave packet and for the four symmetry species [Eq. (5)]. The five correlation functions were then used to construct the corresponding Hamiltonian and overlap matrices [Eqs. (8) and (9)] [25] that were subsequently diagonalized via a generalized eigensolver [29]. The results are denoted as either filter diagonalization (FD) or symmetry-adapted filter diagonalization (SAFD).

The lowest 20 converged eigenvalues of the discretized Hamiltonian are listed in Table I along with their symmetry assignment. The ground level is of $(++)$ symmetry and well separated from the excited levels. The excited levels appear to form four-component clusters, which become increasingly degenerate as energy increases. The fourfold near degeneracy can be attributed to the permutation and inversion symmetries of the system and to the weak coupling between the two electrons. The autocorrelation functions were calculated using projected propagation states [first part of Eq. (5)] to facilitate the doubling of the propagation steps [cf. Eq. (6)]. For $2K=3000$, all the eigenvalues below $-1.5$ were converged beyond seven significant figures. The convergence with other adjustable filtering parameters was also checked.

The convergence rate of filter diagonalization with respect to the number of propagation steps is primarily determined by the smallest energy gap in the spectrum. In Fig. 1, the energy gap between two adjacent levels ($\Delta E_n=E_n-E_{n-1}$) is plotted as a function of energy for the overall spectrum (upper panel) and for each of the four symmetry species (lower panel). The smallest energy gap ($\Delta E=3.8\times10^{-6}$ a.u.) for the overall spectrum occurs near $E=-1.7288$ a.u. between two nearly degenerate states with different symmetries. This diminishingly small energy gap becomes a bottleneck for the conventional spectral analysis. Indeed, the 70th and 71st states cannot be resolved using the conventional filter diagonalization even for the longest propagation ($2K=32\,000$) carried out by us. As shown in Table II, only one of them can be identified. (The error listed in this and the next tables is defined as the difference between an eigenvalue and the corresponding ''exact'' value, which is obtained with SAFD and $2K=32\,000$.) This should not come as a surprise because such a fine resolution would require $\sim10^6$ Chebyshev propagation steps according to the uncertainty principle.

On the other hand, the energy gap for the symmetry-adapted spectra, as shown in Fig. 1(b), is typically much larger than that of the overall spectrum. This is because the symmetry decomposition removes much of the four-fold near degeneracy. For the two states discussed in Table II, for example, the SAFD had no problem in converging them and only about one-tenth of propagation steps were needed.

Interestingly, the energy gaps for all four symmetry species in this model fall roughly on a single curve, as shown in Fig. 1(b). This can be attributed to the weak coupling between the two electrons and the resulting degeneracy. The smallest gap occurs at $E=-1.9315$ a.u. between two $(++)$ (21st and 24th) states. This energy gap ($\Delta E=4.0\times10^{-3}$ a.u.) is approximately three orders of magnitude larger than the smallest gap of the overall spectrum. Therefore, much fewer Chebyshev steps were needed to converge the eigenvalues. Table III presents some data to illustrate the convergence with respect to the propagation steps for four states in the vicinity of the energy. It is obvious that the SAFD converges significantly faster than the conventional FD. The results in Tables II and III indicate that the symmetry-adapted filter diagonalization can at least reduce the computationalcost by a factor of five for this system.

TABLE II. Convergence with respect to $2K$ for two levels with the smallest energy gap in the overall spectrum. The symmetry-adapted filter diagonalization and conventional filter diagonalization are denoted as SAFD and FD, respectively.

| | Energy (a.u.) | $\delta E$ (SAFD) $2K=1600$ | $\delta E$ (SAFD) $2K=2000$ | $\delta E$ (FD) $2K=16\,000$ | $\delta E$ (FD) $2K=32\,000$ |
|---|---|---|---|---|---|
| $E_{70}$ | $-1.728\,815\,305\,597$ | $-2.4\times10^{-7}$ | $-7\times10^{-12}$ | Missed | Missed |
| $E_{71}$ | $-1.728\,811\,496\,969$ | $3.6\times10^{-6}$ | $3.0\times10^{-9}$ | $-7.2\times10^{-9}$ | $-8.0\times10^{-8}$ |

TABLE III. Convergence with respect to $2K$ for four levels near $E=-1.93$ a.u. (see text). The symmetry-adapted filter diagonalization and conventional filter diagonalization are denoted as SAFD and FD, respectively.

| | Energy (a.u.) | $\delta E$ (SAFD) $2K=2500$ | $\delta E$ (SAFD) $2K=3000$ | $\delta E$ (FD) $2K=16\,000$ | $\delta E$ (FD) $2K=20\,000$ |
|---|---|---|---|---|---|
| $E_{20}$ | −1.935 914 824 370 | $2.3\times10^{-8}$ | $-1.5\times10^{-9}$ | $-1.5\times10^{-7}$ | $5.0\times10^{-11}$ |
| $E_{21}$ | −1.935 523 855 470 | $-1.7\times10^{-5}$ | $2.1\times10^{-9}$ | $-8.8\times10^{-7}$ | $3.7\times10^{-10}$ |
| $E_{23}$ | −1.931 892 900 658 | $6.2\times10^{-8}$ | $3.8\times10^{-9}$ | $1.3\times10^{-5}$ | $3.9\times10^{-8}$ |
| $E_{24}$ | −1.931 510 559 410 | $2.3\times10^{-5}$ | $-1.0\times10^{-9}$ | Missed | $2.2\times10^{-6}$ |

## IV. CONCLUSION

Many physical systems possess certain types of symmetry. It is thus important to take advantage of the symmetry in numerical calculations, particularly for large systems and for highly excited states. We have shown in this work that the spectral analysis can be enhanced by symmetry adaptation. In our method, only a single wave packet is propagated and the symmetry components are obtained by using projection operators along the propagation. Hence, the propagation of multiple symmetry-adapted wave packets is avoided. The numerical results clearly demonstrated that symmetry adaptation can significantly improve convergence. There are two major reasons for the symmetry enhancement. First, the density of states in each symmetry species is reduced on average by a factor of $M$ ($M=4$ for the numerical test). The $M$-factor scaling law typically cuts the number of propagation steps to $1/M$. Second and sometimes more importantly, the symmetry decomposition removes the symmetry-induced near degeneracy responsible for the slow convergence in the spectral analysis with no symmetry adaptation. The removal of the near degeneracy results in an additional improvement in numerical efficiency over the $M$-factor scaling law.

A different way to understand the enhancement is to compare the scheme suggested here with the block method in which a number of initial states is propagated simultaneously [33,34]. In our method, the propagation of multiple symmetry-adapted wave packets is implicitly executed by the propagation of a single wave packet. This is possible because the symmetry components are mutually orthogonal and the projection operators commute with the propagator. In this sense, our scheme is an implicit block method that has the advantage of the block method but costs less. Of course, the symmetry adaptation can also be applied to the block method to enhance its own efficiency.

Admittedly, the model used to illustrate the method is oversimplified. However, the results reported for this numerical prototype are encouraging and revealing. Calculations with larger systems, such as the vibrational spectrum of planar acetylene, are currently underway and symmetry enhancement has been found to be significant. The results will be published elsewhere [35].

## ACKNOWLEDGMENTS

This work was supported by the National Science Foundation (Grant No. CHE-9713995), and by the Petroleum Research Fund administered by the American Chemical Society.

[1] R. Kosloff, J. Phys. Chem. **92**, 2087 (1988).
[2] R. Kosloff, Annu. Rev. Phys. Chem. **45**, 145 (1994).
[3] R. Chen and H. Guo, J. Chem. Phys. **108**, 6068 (1998).
[4] R. Chen and H. Guo, J. Chem. Phys. **105**, 3569 (1996).
[5] C. Lanczos, J. Res. Natl. Bur. Stand. **45**, 255 (1950).
[6] H. Tal-Ezer and R. Kosloff, J. Chem. Phys. **81**, 3967 (1984).
[7] R. Kosloff and H. Tal-Ezer, Chem. Phys. Lett. **127**, 223 (1986).
[8] Y. Huang, W. Zhu, D. Kouri, and D. K. Hoffman, Chem. Phys. Lett. **206**, 96 (1993).
[9] W. Zhu, Y. Huang, D. J. Kouri, C. Chandler, and D. K. Hoffman, Chem. Phys. Lett. **217**, 73 (1994).
[10] V. A. Mandelshtam and H. S. Taylor, J. Chem. Phys. **102**, 7390 (1995).
[11] R. N. Silver and H. Röder, Phys. Rev. E **56**, 4822 (1997).
[12] E. J. Heller, J. Chem. Phys. **68**, 2066 (1978).
[13] M. D. Feit, J. A. Fleck, and A. Steger, J. Comput. Phys. **47**, 412 (1982).
[14] A. Messiah, *Quantum Mechanics* (Wiley, New York, 1968).
[15] D. Neuhauser, J. Chem. Phys. **93**, 2611 (1990).
[16] D. Neuhauser, J. Chem. Phys. **95**, 4927 (1991).
[17] R. Chen and H. Guo, J. Chem. Phys. **105**, 1311 (1996).
[18] V. A. Mandelshtam, T. P. Grozdanov, and H. S. Taylor, J. Chem. Phys. **103**, 10 074 (1995).
[19] V. A. Mandelshtam and H. S. Taylor, J. Chem. Soc., Faraday Trans. **93**, 847 (1997).
[20] P.-N. Roy and T. Carrington, J. Chem. Phys. **103**, 5600 (1995).
[21] R. Chen and H. Guo, Chem. Phys. Lett. **261**, 605 (1996).
[22] M. R. Wall and D. Neuhauser, J. Chem. Phys. **102**, 8011 (1995).
[23] V. A. Mandelshtam and H. S. Taylor, J. Chem. Phys. **106**, 5085 (1997).
[24] V. A. Mandelshtam and H. S. Taylor, Phys. Rev. Lett. **78**, 3274 (1997).
[25] R. Chen and H. Guo, Chem. Phys. Lett. **279**, 252 (1997).
[26] L. Liu and J. T. Muckerman, J. Chem. Phys. **107**, 3402 (1997).
[27] G. C. Schatz and M. A. Ratner, *Quantum Mechanics in Chemistry* (Prentice-Hall, Englewood Cliffs, NJ, 1993).

[28] V. Engel, Chem. Phys. Lett. **189**, 76 (1992).
[29] B. S. Garbow, J. M. Boyle, J. J. Dongarra, and C. B. Moler, *Matrix Eigensystem Routines—EISPACK Guide Extension* (Springer-Verlag, New York, 1977).
[30] R. Grobe and J. H. Eberly, Phys. Rev. Lett. **68**, 2905 (1992).
[31] D. Bauer, Phys. Rev. A **56**, 3028 (1997).
[32] D. Kosloff and R. Kosloff, J. Comput. Phys. **52**, 35 (1983).
[33] R. G. Grimes, J. G. Lewis, and H. D. Simon, SIAM J. Matrix Anal. Appl. **15**, 228 (1994).
[34] T. J. Minehardt, J. D. Adcock, and R. E. Wyatt, Phys. Rev. E **56**, 4837 (1997).
[35] R. Chen, H. Guo, L. Liu, and J. Muckerman, J. Chem. Phys. (to be published).